



Quaternary paleoceanography of the central Arctic based on Integrated Ocean Drilling Program Arctic Coring Expedition 302 foraminiferal assemblages

Thomas M. Cronin,¹ Shannon A. Smith,¹ Frédérique Eynaud,² Matthew O'Regan,³ and John King³

Received 30 April 2007; revised 30 November 2007; accepted 2 January 2008; published 22 March 2008.

[1] The Integrated Ocean Drilling Program (IODP) Arctic Coring Expedition (ACEX) Hole 4C from the Lomonosov Ridge in the central Arctic Ocean recovered a continuous 18 m record of Quaternary foraminifera yielding evidence for seasonally ice-free interglacials during the Matuyama, progressive development of large glacials during the mid-Pleistocene transition (MPT) \sim 1.2–0.9 Ma, and the onset of high-amplitude 100-ka orbital cycles \sim 500 ka. Foraminiferal preservation in sediments from the Arctic is influenced by primary (sea ice, organic input, and other environmental conditions) and secondary factors (syndepositional, long-term pore water dissolution). Taking these into account, the ACEX 4C record shows distinct maxima in agglutinated foraminiferal abundance corresponding to several interglacials and deglacials between marine isotope stages (MIS) 13–37, and although less precise dating is available for older sediments, these trends appear to continue through the Matuyama. The MPT is characterized by nearly barren intervals during major glacials (MIS 12, 16, and 22–24) and faunal turnover (MIS 12–24). Abundant calcareous planktonic (mainly *Neogloboquadrina pachyderma* sin.) and benthic foraminifera occur mainly in interglacial intervals during the Brunhes and very rarely in the Matuyama. A distinct faunal transition from calcareous to agglutinated foraminifera 200–300 ka in ACEX 4C is comparable to that found in Arctic sediments from the Lomonosov, Alpha, and Northwind ridges and the Morris Jesup Rise. Down-core disappearance of calcareous taxa is probably related to either reduced sea ice cover prior to the last few 100-ka cycles, pore water dissolution, or both.

Citation: Cronin, T. M., S. A. Smith, F. Eynaud, M. O'Regan, and J. King (2008), Quaternary paleoceanography of the central Arctic based on Integrated Ocean Drilling Program Arctic Coring Expedition 302 foraminiferal assemblages, *Paleoceanography*, 23, PA1S18, doi:10.1029/2007PA001484.

1. Introduction

[2] The Arctic Ocean plays a key role in climate through its contribution to formation and export of North Atlantic Deep Water [Aagaard and Carmack, 1994], its influence on Earth's albedo through changing sea ice cover [Serreze *et al.*, 2007], and export of fresh water from river inflow and melting ice to the North Atlantic [Peterson *et al.*, 2006]. Despite recent advances in Quaternary Arctic paleoceanography back to marine isotope stage 7 (MIS 1–7) [Jakobsson *et al.*, 2001; Backman *et al.*, 2004; Polyak *et al.*, 2004; Spielhagen *et al.*, 2004; Wollenburg *et al.*, 2004; Darby *et al.*, 2006], relatively little is known about Arctic Ocean circulation, sea ice, and freshwater export during major climate changes of the mid and early Quaternary including the mid-Pleistocene transition \sim 1.2 to 0.9 Ma (MPT) [Berger and Jansen, 1994; Raymo *et al.*, 1997; Clark *et al.*, 2006].

[3] On the basis of mainly lithostratigraphic changes showing 19 glacial-interglacial cycles on the Northwind Ridge, Phillips and Grantz [1997] proposed the mid-Pleistocene transition was characterized by increased sediment flux from glacial ice beginning in their cycle 10. Kristoffersen *et al.* [2004] also inferred from geophysical studies of the Lomonosov Ridge and correlations to Ocean Drilling Program (ODP) sites 901 and 911 on the Yermak Plateau [Thiede and Myhre, 1996; Flower, 1997] that deep-draft iceberg armadas embedded in sea ice may have been initiated during the MPT. However, the lack of long sediment cores and conventional paleoceanographic proxies (e.g., calcareous microfossils) and controversy about sedimentation rates and chronology have prevented more definitive assessment of the Quaternary evolution of glacial-interglacial cycles during the MPT in the central Arctic. This is particularly important given changes in global climatic patterns during the MPT, documented extensively in marine and terrestrial paleoclimate records.

[4] Here we use Integrated Ocean Drilling Program (IODP) Arctic Coring Expedition (ACEX) Site M0004, Hole C (hereinafter ACEX 4C) from the Lomonosov Ridge in the central Arctic Ocean (Figure 1, 87°52.065'N, 136°11.381'E and 1287.9 m water depth) [Backman *et al.*, 2006; Moran *et al.*, 2006] to investigate Arctic Quaternary

¹U.S. Geological Survey, Reston, Virginia, USA.

²Laboratoire Environnements et Paléoenvironnements Océaniques, UMR CNRS 5805, Université Bordeaux I, Talence, France.

³Graduate School of Oceanography, University of Rhode Island, Narragansett, Rhode Island, USA.

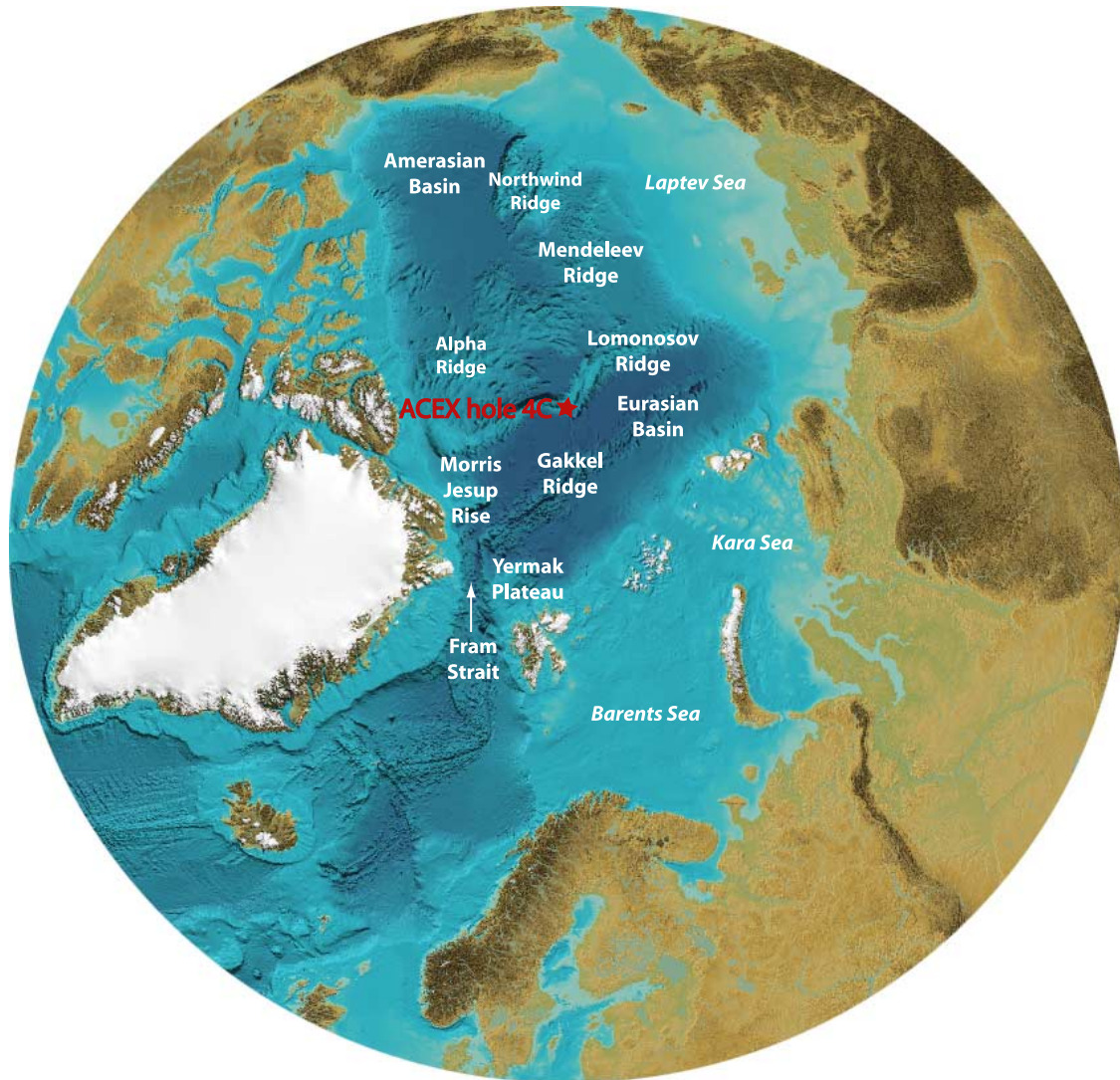


Figure 1. Map showing location of ACEX 4C and other regions studied for Quaternary foraminifers. Base map from M. Jakobsson.

paleoceanography during the past 1.5 Ma. We focus on three topics: (1) the progressive down-core disappearance of calcareous microfossils and appearance of agglutinated benthic foraminifers (ABF), a pattern observed at ACEX 4C, as well as other ridges in the Arctic Ocean, (2) changes in ABF abundance and bulk sediment density before, during, and after the MPT, and (3) the changes in ABF assemblage composition during MPT. The results have implications for both Quaternary oceanographic changes in the Arctic and also for future coring strategy.

2. Material and Methods

2.1. ACEX Samples

[5] We studied 301 foraminiferal samples from ACEX 4C cores 1H1 to 6X1 with emphasis on the uppermost 18 m (revised composite depth scale (rmcd)) [O'Regan *et al.*, 2008]. We processed 2-cm-thick samples every 5 to 10 cm as follows: sediment samples were weighed, dried overnight

and then weighed again to compute foraminiferal abundance. Processing was carried out for the first 203 samples in Environnements et Paléoenvironnements Océanique (EPOC) Laboratory, Université de Bordeaux) and an additional 98 samples at the U. S. Geological Survey (USGS) in Reston, Virginia. Sediments were washed through a 125 μm sieve at EPOC and those at USGS through a 63 μm sieve. Planktonic and benthic foraminifers were picked and identified from the >125 μm size fraction.

2.2. Arctic Foraminiferal Methods

[6] The choice of size fraction can be important in foraminiferal analyses, especially in sediments from the Arctic Ocean. Schröder *et al.* [1987] compared results using >63 and >125 μm fractions and showed the main difference was in calcareous foraminiferal assemblages where the abundance of two small taxa, *Stetsonia*, and *Epistominella*, dominate the fine fraction. Such dominance occurs mainly in the Arctic's abyssal plains, not on ridges like the Lomo-

nosov Ridge. *Nørgaard-Pedersen et al.* [2007] also showed that the 63–125 μm fraction is important in analyses of planktonic foraminifers from the Arctic as this is where *Turborotalita quinqueloba*, a species useful for sea ice reconstructions, is most abundant.

[7] The majority of down-core Arctic benthic foraminiferal studies either picked and/or analyzed the >125 μm size fraction [*Poore et al.*, 1994; *Ishman et al.*, 1996; *Osterman et al.*, 1999; *Polyak et al.*, 2004]. *Poore et al.* [1994] concluded that the >125 μm size fraction was representative of that from 63–125 μm . *Ishman et al.* [1996] used the >150 μm size fraction for foraminiferal analysis and >100 μm for assemblages in western Arctic Northwind and Mendeleev ridges. In studies of the Mendeleev Ridge, *Polyak et al.* [2004] analyzed 60 samples for >150 μm and 19 for >63 μm in the calcareous facies. In a study of ODP Leg 105 (Baffin Bay, Labrador Sea) foraminifers, *Kaminski et al.* [1989] examined the 63–125 μm fraction only in calcareous facies. *Wollenburg et al.* [2001] ran multivariate analyses on the >125 μm fraction from R/V *Polarstern* core PS-2212 (Yermak Plateau) to minimize bias from carbonate dissolution. *Scott et al.* [1989] studied >63 μm CESAR core 14 from the Alpha Ridge and found mainly *Cyclammina*, a large taxon, was dominant (50–100%) below 250 cm core depth which is below calcareous foraminiferal facies (see below). *Evans* [1998] [see also *Evans and Kaminski*, 1998] conducted the most comprehensive studies of Quaternary Arctic agglutinated foraminifers from many regions of the Arctic Ocean. Among his conclusions, the 63–125 μm fraction was usually barren of foraminifers, and when present composed only 2–6% of the total assemblage. The 63–125 μm fraction consists almost exclusively of specimens of *Glomospira*, an ecologically insignificant genus.

[8] We picked foraminifera from the 63–125 μm fraction from two intervals, 9.82 to 11.33 mcd and 16.01 to 17.51 mcd, to evaluate the importance of this size fraction in ACEX 4C. Eight of 11 samples were barren of fine foraminifers. One sample had 12 *Glomospira*; the other seven had a total of only 10 specimens in the 63–125 μm fraction composing 9.6% of the total assemblage from all size fractions in these samples. We also scanned the 63–125 μm size fraction at levels below the oldest calcareous zones and confirmed that agglutinated foraminifera were absent or rare and often fragmented. The same observation was made on planktonic foraminifers with no occurrences of *T. quinqueloba* in the 63–125 μm size fraction.

[9] In sum, except for thin, intermittent calcareous zones from the uppermost 2–3 m on Arctic submarine ridges, small foraminifers occur in the <125 μm size fraction of the ACEX cores but in very low numbers as is true elsewhere in the Arctic. An exception is the Barents Sea slope region, eastern Arctic, where foraminiferal preservation is generally excellent [*Wollenburg et al.*, 2001]. Primary and postmortem processes influencing foraminiferal assemblages are discussed below.

[10] In addition to ACEX 4C assemblages, we restudied the benthic foraminiferal data from shorter cores from previous studies of the Lomonosov, Alpha, Mendeleev, and Northwind ridges and the Morris Jesup Rise in an effort

to evaluate Arctic-wide biostratigraphy and preservation patterns of calcareous and agglutinated taxa (Figure 1 and Table 1). These analyses included the first study of agglutinated foraminiferal assemblages from below 280 cm in core 96/12 from the Lomonosov Ridge [*Jakobsson et al.*, 2001]. This level marks the disappearance of calcareous foraminifers and dominance of agglutinated taxa (L. Polyak, personal communication, 2007). We followed the taxonomy of *Evans and Kaminski* [1998], *Evans et al.* [1995], and *Osterman and Spiegler* [1996]. All foraminiferal data are available at the National Paleoclimatic Data Center (<http://www.ncdc.noaa.gov/paleo/paleo.html>) and at the IODP-MSP archive (Publishing Network for Geoscientific and Environmental Data (PANGAEA)).

3. ACEX 4C Lithostratigraphy, Sedimentation Rates, and Chronology

3.1. Lithostratigraphy

[11] Using cores taken from ice islands, *Clark et al.* [1980] recognized 13 lithostratigraphic units in the uppermost several meters of sediment from the central Arctic Ocean (units A–M). These units have been recognized across a large part of the Arctic Ocean [*Clark*, 1990; *Scott et al.*, 1989; *Phillips and Grantz*, 2001]. *Phillips and Grantz* [1997] expanded on *Clark et al.*'s lithostratigraphic framework and showed that Quaternary sediments deposited on ridges in the Arctic generally consist of ochre (brown units to some authors), pelagic calcareous muds, often bioturbated and containing ice-rafted dropstones and calcareous microfossils, alternating with laminated olive-grey muds and sands usually barren of calcareous microfossils and glacial erratics. The ochre and grey facies are generally considered representative of interglacial and glacial sediments respectively. Nineteen such glacial-interglacial cycles have been identified on the Northwind Ridge [*Phillips and Grantz*, 1997].

[12] In addition to their distinct color and lithological characteristics, interglacial-glacial cycles on the Lomonosov Ridge are characterized by cyclic variations in manganese concentrations during the Brunhes [*Jakobsson et al.*, 2000]. Depending on the location of the core, the uppermost sediments also exhibit large changes in grain size, bulk density, magnetic inclination, and mineralogy of ice-rafted debris [e.g., *Bischof et al.*, 1996; *Jakobsson et al.*, 2001; *Phillips and Grantz*, 2001; *Darby et al.*, 2006]. It should also be emphasized that high-resolution analyses of cores using multiple proxies indicate complex lithological and paleoceanographic changes during the transitions from glacial to interglacial regimes [*Phillips and Grantz*, 1997; *Spielhagen et al.*, 2004; *Wollenburg et al.*, 2004].

3.2. Dating and Correlation of Arctic Sediments

[13] Radiocarbon dating of Arctic sediments has provided an improved chronology for Arctic paleoceanographic reconstructions of the last glacial maximum, the deglacial and the Holocene interglacial period [*Stein et al.*, 1994; *Poore et al.*, 1999; *Nørgaard-Pedersen et al.*, 2003; *Spielhagen et al.*, 2004]. On the Barents Sea slope, *Matthiessen et al.* [2001] used dinoflagellate cysts and *Wollenburg et al.* [2001] used foraminifers and stable isotopes to reconstruct the paleoceanographic history of the past 150,000 years

Table 1. Core Data for Arctic Ocean Foraminiferal Data

Core	Location	Platform	Latitude	Longitude	Water Depth, m	Sources
ACEX M00004 Hole 4C	Lomonosov Ridge	Vidar Viking	87°52.065'N	136°11.381'E	1287.9	this paper
PS2177-5	Lomonosov Ridge	Polarstern	88°02.10'N	134°36.7'E	1400	Fütterer [1992], Evans and Kaminski [1998]
PS2200-5	Morris Jesup Rise	Polarstern	85°19.40'N	14°00.00'W	1073	Fütterer [1992], Evans and Kaminski [1998]
PS2185-6	Lomonosov Ridge	Polarstern	87°32.20'N	144°55.60'E	1052	Fütterer [1992], Evans and Kaminski [1998]
PI-92-AR21	Northwind Ridge	Polar Star	76°51.80'N	154°12.86'E	951	Phillips and Grantz [2001]
PI-92-AR27	Northwind Ridge	Polar Star	74°00.00'N	157°36.54'W	1214	Evans [1998]
PI-92-AR30	Northwind Ridge	Polar Star	75°18.70'N	158°02.78'W	765	Phillips and Grantz [2001]
PI-92-AR39	Northwind Ridge	Polar Star	75°50.65'N	156°01.92'W	1470	Evans [1998]
PI88-AR-3	Northwind Ridge	Polar Star	74°35.6'N	157°39.59'W	1909	Phillips and Grantz [1997], Poore et al. [1993], Ishman et al. [1996]
PI88-AR-5	Northwind Ridge	Polar Star	74°37.35'N	157°53.04'W	1089	Phillips and Grantz [1997], Poore et al. [1993], Ishman et al. [1996]
NP-26-5	Mendeleev Ridge	Ice station Severnyj Polyus	78°59'N	178°07'W	1435	Ishman et al. [1996], Polyak et al. [2004]
NP-26-32	Mendeleev Ridge	Ice station Severnyj Polyus	79°24'N	178°05'W	1610	Ishman et al. [1996], Polyak et al. [2004]
CESAR-14	Alpha Ridge	CESAR ice camp	85°51'N	108°21.6'W	1370	Scott et al. [1989]
96/12-pe1	Lomonosov Ridge	Oden	87°05.9'N	144°46.4'E	1003	this paper, Jakobsson et al. [2000], Backman et al. [2004]

with radiocarbon, isotopic and paleomagnetic methods for chronology.

[14] In regions other than the Barents Sea–Spitzbergen margin, chronology for sediments too old for radiocarbon dating has been a persistent problem because of the lack of calcareous microfossils for oxygen isotopic analysis and conflicting interpretations about paleomagnetic reversals [see Polyak et al., 2004; Jakobsson et al., 2001; Spielhagen et al., 2004, Schneider et al., 1996; Backman et al., 2004]. The “long” chronology [Clark, 1970; Clark et al., 1980; Scott et al., 1989; Spielhagen et al., 1997] holds that changes in magnetic polarity in the uppermost few meters signify Pliocene and Quaternary polarity reversals such as the Gauss/Gilbert, Brunhes/Matuyama and other boundaries. This interpretation, called the “sediment starved” model by Backman et al. [2004], implies very low mean sedimentation rates ($\sim 1 \text{ mm ka}^{-1}$) during the past several million years in much of the Arctic Ocean.

[15] More recently, a consensus has emerged, based on biostratigraphic (especially calcareous nannofossils) and paleomagnetic data, in which observed polarity changes at many sites in the Arctic are considered to be short-lived paleomagnetic excursions during the Brunhes [Nowaczyk and Baumann, 1992; Frederichs, 1995; Jakobsson et al., 2000]. This interpretation holds that the Arctic Ocean is not a sediment-starved basin and, although rates vary significantly in time and space, a mean long-term sedimentation rate of about 1 cm ka^{-1} fits the majority of available data [Backman et al., 2004].

[16] Our study is focused on the last 1.5 Ma of Quaternary sedimentation, but it is important to confirm the age of the uppermost 25 cm of calcareous facies with radiocarbon dating. Table 2 gives data on four samples of *Neoglobobulimina pachyderma* (mostly sinistral) picked from the $>125 \mu\text{m}$ size fraction. The results show that two sample ages could be calibrated using INTCAL04 marine calibration with standard 400-year mean global reservoir correction and no local ΔR correction are 3–5 cm: 6025–6263 years (2-sigma range), and 18–20 cm: 24,861–25,575 years. This older age must be viewed with caution as reservoir effects in the Arctic Ocean are unknown and likely large. Similar reservoir problems are probably associated with the two uncalibrated ages (26.2 and 36.7 ka), which are beyond the INTCAL04 calibration curve and also suffer from unknown reservoir effects. These uncertainties are due partly to the complexity of the global carbon cycle and changes in ^{14}C production during the interval 40–20 ka [Beck et al., 2001; Hughen et al., 2004] and the importance of sea ice and local carbon cycle effects in high-latitude seas [Voelker et al., 1998]. Despite these uncertainties the upper 30 cm of ACEX 4C is clearly correlative with late MIS 3, MIS 2 and MIS 1 and younger than the last interglacial MIS 5e.

3.3. ACEX Age Model

[17] The age model for ACEX 4C data is described in detail by O'Regan et al. [2008]. They show that multiple proxies (bulk density, magnetic grain size proxies and color variation) for what have traditionally been interpreted as ‘glacial/stadial’ and ‘interglacial/interstadial’ depositional modes in the central Arctic Ocean have significant spectral power at

Table 2. ACEX 302 Radiocarbon Dates on *N. pachyderma*^a

Sample	Depth ^b (cm)	$\delta^{13}\text{C}$ (‰)	Radiocarbon Age (years B.P.)	Error	Cal Age	Cal Age Range (2 σ)
60698	3	0.76	5740	40	6,164.5	6,106–6,223
60699	18	0.34	21,400	100	2,5218	24,861–25,575
60700	23	0.83	36,700	320	NA	NA
60701	38	0.65	26,200	130	NA	NA

^aAll dates from *Neogloboquadrina pachyderma* from ACEX 302 Hole 4C Core 1, Section 1. Calibrated (Cal) age computed from CALIB radiocarbon calibration program CALIB 5.01 [see *Stuiver and Reimer, 1993; Hughen et al., 2004*]. Dates from National Ocean Sciences Accelerator Mass Spectrometry (NOSAMS).

^bTop depth 2-cm-thick sample.

predicted Milankovitch frequencies. This observation has been used in conjunction with limited Pleistocene biostratigraphic markers and the broad constraints provided by the magnetic inclination record to propose a Pleistocene age model extending back to 1.2 Ma. However, the limited number of biostratigraphic markers, poor overlap in the deeper sections, complexity of the magnetic inclination record and questions concerning the correct tuning target add uncertainty to the proposed age model. To account for these errors O'Regan et al. use a series of possible solutions to describe an error envelope for the age model, the magnitude of which varies through time. For the Pleistocene, the average range of error is reported as 27 ka (maximum error range 87 ka). Although pronounced cyclicity in the proxy data continues into the Pliocene, increased uncertainty in an appropriate tuning target (i.e., global ice volume versus insolation) prevents an unambiguous age model from being derived.

[18] For the late Quaternary (MIS 1–6), ages were mapped onto the ACEX composite record from the detailed chronostratigraphy of proximal piston cores collected from circumpolar regions of the Lomonosov Ridge [Jakobsson et al., 2000, 2001, 2003; Spielhagen et al., 2004] and supplemented with ¹⁴C dates from ACEX 4C. The cyclostratigraphic solution for MIS 6–21 closely corresponds to a previous cyclostratigraphic age model presented for a 7.22-m-long piston core (96/12-PC) recovered from the central Lomonosov Ridge in 1996 [Jakobsson et al., 2000]. For this interval, the reported error allows the identification of individual MIS stages, but cannot be used to resolve the terminations of the glacial cycles. Beyond MIS 36/37 (~1.2 Ma), the ACEX 4C record provides a unique glimpse into paleoceanographic changes during the Matuyama but cannot be used to positively differentiate between individual MIS stages.

[19] Overall results from the age model suggest a mean sediment accumulation rate of ~1.3 cm ka⁻¹ for the Quaternary at this site on the Lomonosov Ridge. This mean sedimentation rate is slightly lower than the average Neogene estimate of 1.45 cm ka⁻¹ estimated by Frank et al. [2008] and Backman et al. [2008]. This age model yields an approximate foraminiferal sampling resolution ranging from ~5 to 15 ka.

4. Arctic Foraminiferal Ecology and Preservation

4.1. Modern Arctic Benthic Foraminifera

[20] We briefly review some of the literature on modern Arctic Ocean foraminifera, their preservation in bottom

sediments and potential for paleoceanographic study. Modern benthic foraminifera have been studied from many parts of the Eurasian and Amerasian Basins of the Arctic Ocean and adjacent subpolar seas [Green, 1960; Lagoe, 1977, 1979; Schröder-Adams et al., 1990; Scott and Vilks, 1991; Bergsten, 1994; Hald and Steinsund, 1996; Osterman et al., 1999; Wollenburg and Mackensen, 1998; Wollenburg and Kuhnt, 2000]. The ecology of calcareous taxa allowed the reconstruction of late Quaternary paleocirculation patterns [Poore et al., 1993, 1994; Ishman et al., 1996; Osterman, 1996; Polyak et al., 2004].

[21] In addition to efforts to infer Arctic paleocirculation, Wollenburg and Kuhnt [2000] used quantitative analyses of living versus dead foraminifera in surface sediments to develop a benthic foraminiferal accumulation rate (BFAR) index having potential to evaluate productivity and other aspects of Arctic paleoceanography. In brief, they found that in the modern Arctic, BFAR values are relatively low in seasonally ice-free regions, high under permanent sea ice where calcareous assemblages accumulate, and, importantly, BFAR values are not necessarily related to productivity in a simple way. Wollenburg et al. [2001, 2004] reconstructed a 24-ka paleoproductivity history using a suite of cores from along the margin of the eastern Arctic Ocean. They observed complex changes in BFAR values, as well as other proxies, during the last glacial maximum and deglacial interval, including the Younger Dryas along the Yermak Plateau and Barents Sea slope related to inflowing Atlantic water, sea ice coverage, and other factors.

4.2. Agglutinated Benthic Foraminifera

[22] The predominance of agglutinated benthic foraminifera and the absence of calcareous benthic taxa in surface sediments is a well-documented feature in certain regions of the modern Arctic Ocean. Primary factors related to species' ecology and secondary processes related to selective dissolution of calcareous species are two simple explanations for this phenomenon. Species live under particular environmental conditions to which they are ecologically adapted and their absence might suggest unfavorable conditions at a particular location. In the extreme case, the absence of all benthic faunas in Arctic sediments has suggested to some workers conditions unsuitable for any biological activity, such as during periods of severe ice cover. Conversely, samples barren of foraminifera, or containing only agglutinated species, might reflect postmortem destruction of shells. Wollenburg et al. [2004] demonstrates that multiple factors may contribute to calcareous foraminiferal dissolution. Importantly, agglutinated foraminifera are not immune from postmortem physical and/or chemical destruction

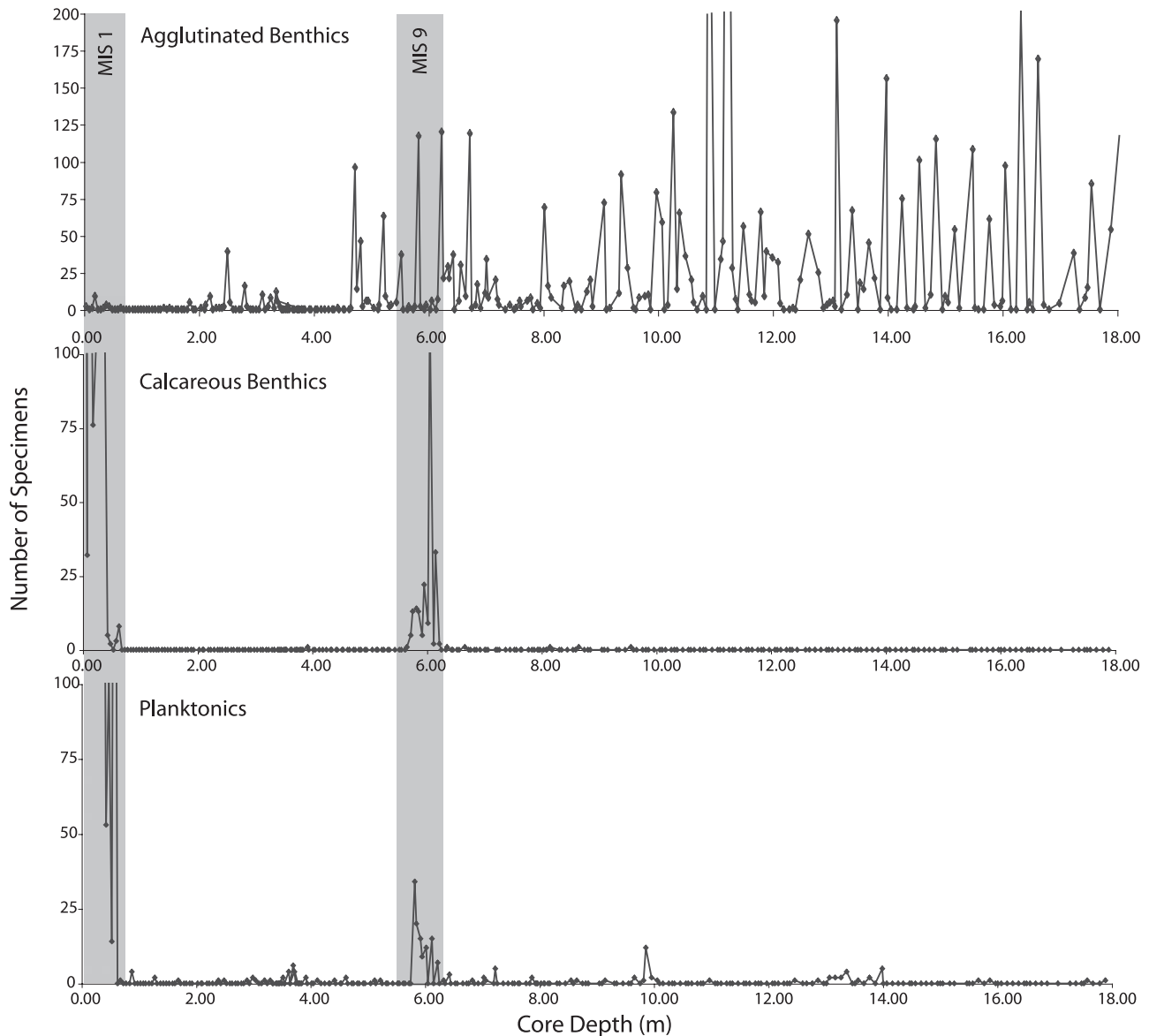


Figure 2. Plot showing abundance of planktonic foraminifers (mostly *Neogloboquadrina pachyderma* sin.), calcareous benthic and agglutinated benthic foraminifers (approximately per 10 g dry weight) for uppermost 18 m of sediment from ACEX 4C. This interval represents the entire Quaternary.

depending on morphology, texture, and type of cement [see Murray and Alve, 1994].

[23] In addition to ecological factors and syndepositional postmortem dissolution, long-term (tens to hundreds of thousands of years) shell dissolution by pore water might also influence down-core preservation. We discuss this possibility below in the context of the stratigraphic distribution of ABFs in Arctic cores.

[24] With these caveats about preservation biases in mind, there is nonetheless substantial evidence that ABF assemblages dominate in surface sediments accumulating in regions of seasonally ice-free conditions, often characterized by brine formation, cold, well oxygenated bottom water, and high organic carbon flux [Scott and Vilks, 1991; Steinsund and Hald, 1994; Evans, 1998; Wollenburg

and Kuhnt, 2000]. Today such regions include highly productive continental shelf and slope regions off Eurasia, parts of Baffin Bay at 1000–2000 m water depth, and the Barents Sea where carbonate dissolution is a major factor influencing foraminiferal preservation.

5. Results

5.1. ACEX 4C Foraminiferal Stratigraphy

[25] Figure 2 plots the abundance of planktonic, benthic calcareous and benthic agglutinated foraminifers against core depth. The results show that (1) abundant calcareous microfossils occur only in the uppermost interval (~ 0.6 mcd at this site versus typically 0.1–0.3 m below seafloor (mbsf) elsewhere), (2) several intervals down core

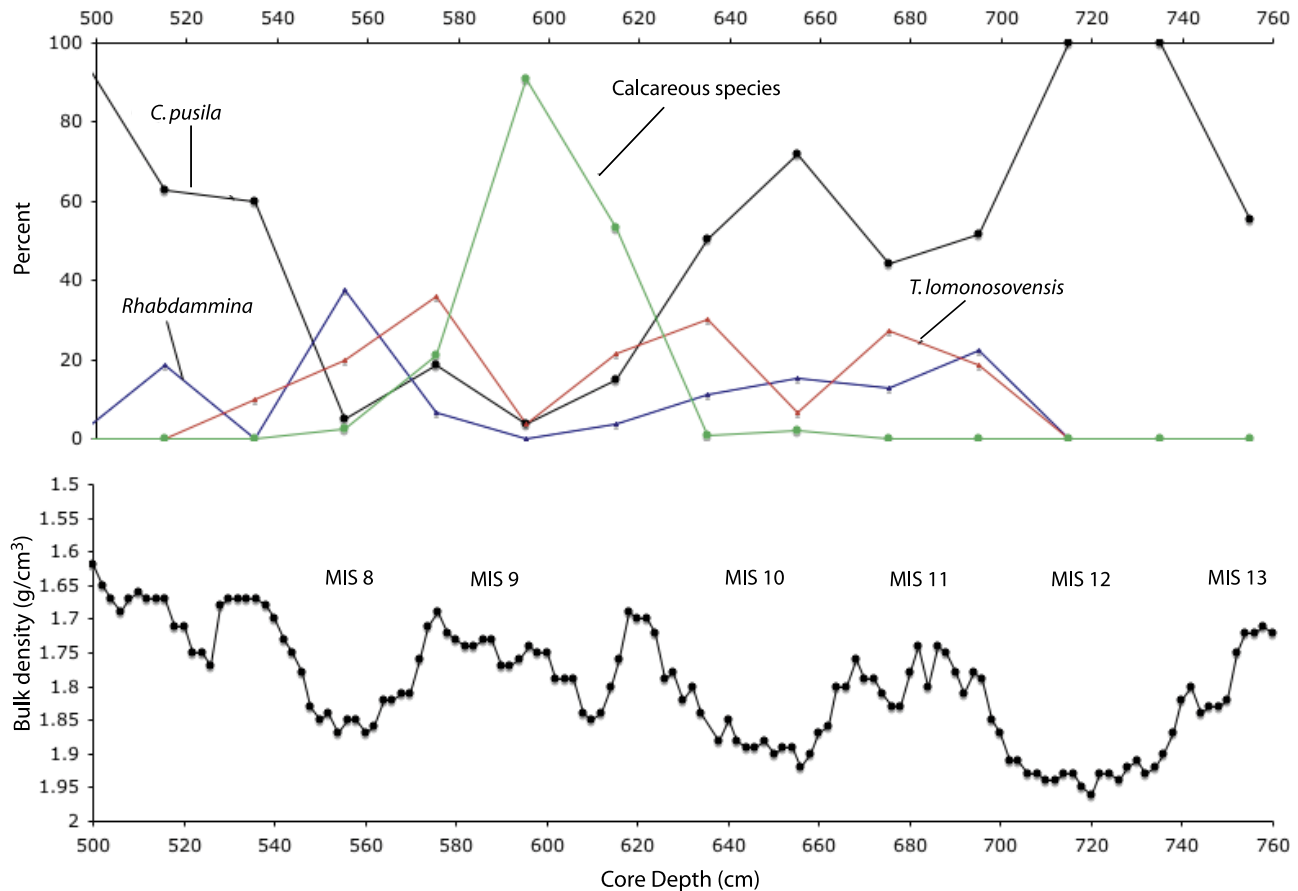


Figure 3. (top) Relative abundance of three common agglutinated species and total calcareous benthic species in ACEX 4C from 7.6 to 5.0 core depth (rmcd). (bottom) Sediment bulk density. Bulk density varies with changes in bulk sediment grain size, with broad lows (highs) in bulk density corresponding to finer (coarser) grain sizes deposited during interglacials (glacials). Marine isotope stages 8–13 are labeled. MIS 9 is the lowest level in ACEX 4C containing abundant calcareous assemblages.

containing common but decreasing numbers of calcareous foraminifers, (3) a transition to agglutinated dominated faunas below ~6.3–4.50 rmcd, (4) planktonic foraminifers are only occasionally found below ~0.7 rmcd but not in sufficient abundance to permit stable isotopic analyses or faunal assemblage analyses, and (5) agglutinated foraminifers occur intermittently, but often in large numbers, down to 18 rmcd.

[26] In the upper 0.7 rmcd, patterns are similar to those observed at other sites on the Lomonosov Ridge and on other ridges in the Arctic. Sediments from below ~700 cm signify new and important aspects to Arctic foraminiferal stratigraphy.

[27] On the basis of the radiocarbon dates and age model [O'Regan *et al.*, 2008], the uppermost 0.6 rmcd represents the MIS 1 (Holocene interglacial), the last deglaciation (Termination 1) and possibly part of MIS 3. The spike in calcareous microfossils centered near 6 rmcd signifies MIS 9. Planktonic assemblages are dominated (>95%) by the sinistral form of *Neogloboquadrina pachyderma* in association with a few dextral specimens. Discrete occurrences of *Turborotalita* (formerly *Globigerina*) *quinqueloba* and some atypical *Globigerina bulloides* occur in the upper

0.6 rmcd. Statistical analyses of distinct morphotypes of *N. pachyderma* sinistral and their taxonomy for populations from the uppermost samples of ACEX 4C are given by Eynaud *et al.* [2008].

[28] The calcareous benthic assemblages are dominated by *Cassidulina teretis*, *C. reniforme*, and *Oridorsalis tener*, with small numbers of *Quinqueloculina* spp., *Planulina wuellerstorfi*, *Haynesina*, *Dentalina*, *Bulimina* and other rare species. These assemblages are generally similar to those found in core 96/12 in the uppermost 0.1 mbsf and in a calcareous-rich zone near 0.2 mbsf [Jakobsson *et al.*, 2001].

[29] A plot of agglutinated and calcareous benthic foraminiferal abundance and sediment bulk density (low bulk density equals interglacials) for the MIS 8–12 interval (Figure 3) shows that calcareous faunas dominate MIS 9, and ABFs dominate MIS 8 (*Rhabdammina* and *Trochammina lomonosovensis*), MIS 10 and MIS 12 (*Cyclammina pusilla*). Calcareous biofacies have been used for late Quaternary Arctic paleoceanography; assemblage composition differs between and within interglacial intervals [Ishman *et al.*, 1996; Polyak *et al.*, 2004; Wollenburg *et al.*, 2004] but there is no standard benthic ecostratigraphy applicable across the Arctic.

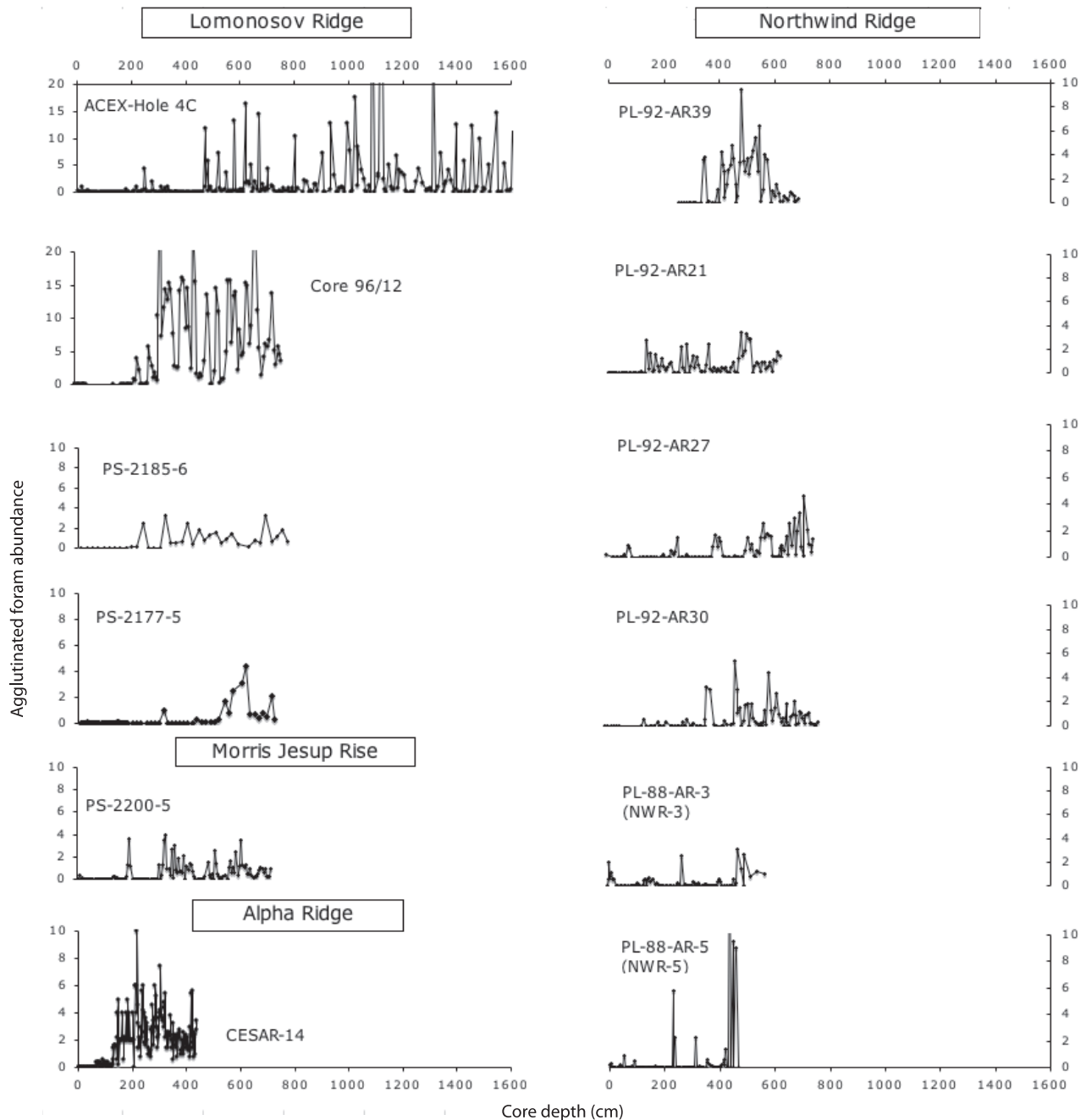


Figure 4. Agglutinated benthic foraminiferal abundance in Arctic cores from Lomonosov, Alpha, and Northwind ridges and Morris Jesup Rise. Table 1 gives site data. These sites range in depth from 765 to almost 1500 cm water depth. The transition from intervals in the upper 200–600 cm with rare to absent ABFs to abundant ABFs is a widespread phenomenon in the Arctic Ocean and is estimated to occur at about MIS 7–9, although age data are limited to ACEX 4C and PS-2185-6 and more limited age data from other sites. Y axis indicates specimens per gram. Values are approximate as picking methods vary slightly among researchers.

5.2. Calcareous-Agglutinated Transition During MIS 7–9

[30] The most pervasive biostratigraphic event in many regions of the Arctic Ocean is the down-core disappearance of calcareous foraminifers and the increased abundance of agglutinated taxa. Figure 4 plots ABF abundance patterns from ACEX 4C and other cores from the Lomonosov,

Alpha, and Northwind ridges in the western Arctic, and the Morris Jesup Rise north of Greenland obtained from several sources (Table 1).

[31] All cores show one or several minor spikes in ABFs in the upper few meters of sediment, then consistently abundant ABFs down core. The transition to ABF-dominated faunas occurs between ~2 and 6 mbsf depending on

the site. We suspect such a pattern is present in the Mendeleev Ridge where well-preserved calcareous assemblages occur in the upper 200 cm [Polyak *et al.*, 2004], but these cores did not penetrate the transition.

[32] Conversely, cores from the eastern Arctic bordering Spitzbergen and the Barents Sea (PS-2138-1 and PS-2212-3) clearly show a different pattern in which ABFs are abundant in some intervals in the Holocene, and calcareous foraminifers are consistently present down to 3–4 mbsf [Wollenburg *et al.*, 2001, 2004]. Similarly, a simple calcareous-agglutinated transition was not observed in core PS-2176-3 from the abyssal plain of the Amundsen Basin at 4363 m water depth [Evans *et al.*, 1995].

[33] Owing to its widespread occurrence in the central and western Arctic Ocean, we now consider whether the calcareous-ABF transition is synchronous at various sites. The age model for ACEX 4C suggests that 4.2 rmcd core depth is equivalent to Marine Isotope Stage 6. The position of the boundary between MIS 6/7 is 4.65 rmcd at the base of a very distinctive coarse-grained interval also present in regional records (i.e., 96/12 and PS-2185). The final calcareous zone centered at 6.2 rmcd falls in MIS 9. Age data of varying quality from cores from the Lomonosov Ridge (PS-2185-6 [Spielhagen *et al.*, 2004] and see also Nørgaard-Pedersen *et al.* [1998] on short core PS-2185-3; 96/12 [Jakobsson *et al.*, 2000, 2001]; and PS-2177-3 [Stein *et al.*, 1994]) and the Morris Jesup Rise [Stein *et al.*, 1994; Cronin *et al.*, 1994] also support an age of MIS 7–9 for the calcareous-ABF transition. Cores from the Northwind Ridge shown in Figure 4 lack chronological data, but the short chronology proposed by Polyak *et al.* [2004] correlating the Mendeleev record with Northwind Ridge core NWR-5 is consistent with this age interpretation. Thus, within the limits of the chronological data and sampling resolution, the calcareous-ABF transition appears to be synchronous on the central Lomonosov Ridge and, though with less certainty, also on other ridges where it has been found. This interpretation suggests sedimentation rates ranging from less than 1 cm ka⁻¹ on the Alpha Ridge to ~2.0–2.5 cm ka⁻¹ on parts of the Lomonosov and Northwind ridges.

5.3. Mid-Pleistocene Transition in the Arctic

[34] The MPT record on the Lomonosov Ridge is characterized by three primary changes in foraminifers. First, ACEX 4C intervals between ~1300 and 1130 cm, representing MIS 22–24, and between ~1100 and 700 cm (rmcd), representing MIS 20 through 12, are characterized by low ABF abundance including many nearly barren samples (Figures 2 and 4).

[35] Second, intervals with distinct maxima in ABF abundance alternate with nearly barren zones (Figure 5). Twenty-seven such maxima (ABF > 5 forams per gram) are shown in Figure 5 in the bottom plot for intervals older than MIS 6; the highest abundances occur below ~10.0 rmcd which is dated at about MIS 20–21. The top plot shows the details of ABF spikes for MIS 8–12 distinguishing those samples with the highest ABF abundances (>10 forams per gram) from those with moderate densities (5–10 forams per gram). Many ABF maxima coincide with intervals of either

relatively low sediment bulk density or decreasing density, which represent a fining of bulk sediment grain sizes [O'Regan *et al.*, 2008] that largely correspond to interglacial and glacial-interglacial transitions.

[36] Although the provisional age model ends at 1.2 Ma (MIS 36/37) at a depth of 16.23 rmcd, and that foraminiferal sampling resolution may have missed some ABF maxima, it is worth noting that between 4.65 and 18 rmcd there are 27 ABF maxima. Given that *N. pachyderma* (sinistral) occurs at 19.33 rmcd, providing a maximum age estimate of ~1.8 Ma (MIS 64/65) for this depth interval, there is an intriguing link between the number of ABF events and the 29 glacial-interglacial cycles between MIS 7 (4.65 rmcd) and this possible location for the MIS 64/65 boundary.

[37] Third, agglutinated assemblage composition changes between 13.0 and 8.0 rmcd in ACEX 4C (Figure 6). *Alveolophragmium polarensis* abundance falls near 11.7 rmcd and *T. lomonosovensis* becomes abundant ~11.5 rmcd. *Psammosphaera* and *Rhabdammina* also fall in abundance between 11.0 and 8.0 rmcd. A similar pattern of faunal events is seen in Core 96/12 supporting the correlation between the two sites given by O'Regan *et al.* [2008]. For example, the disappearance of *A. polarensis* occurs at 600 cm in 96/12; *Psammosphaera* is largely absent above 460 cm, and *Rhabdammina spp* shows a steady decrease in abundance between 515–368 cm. The ACEX 4C faunal changes begin in the interval dated at MIS 22–24.

[38] Evans [1998] suggested that down-core changes in *Rhabdammina* in PS-2185-6 might be related to changes in trophic structure and influx of organic particulate matter. The ecology of *A. polarensis* is not well known but this species is clearly much more abundant in intervals of core PS-2200 from the Morris Jessup Rise than in cores from the central or western Arctic, suggesting it favors regions of seasonally ice-free conditions. Thus its abundance below MIS 22–24 may be related to reduced sea ice.

6. Discussion

[39] We summarize the central Arctic foraminiferal record as follows. From MIS 9 through MIS 1, calcareous benthic sometimes with planktonic foraminifers characterize interglacial intervals; glacial-age sediments are either barren or contain rare agglutinated foraminifers. Interglacial intervals probably had perennial sea ice such as exists in the current interglacial, while some glacial intervals were characterized by large, deep-draft icebergs [Kristoffersen *et al.*, 2004] and/or ice shelves [Polyak *et al.*, 2001]. These are only first-order patterns and do not preclude complex paleoceanographic changes during stadials and interstadials within glacial intervals [Nørgaard-Pedersen *et al.*, 1998; Wollenburg *et al.*, 2001] or millennial-scale climate events during glacial terminations [Poore *et al.*, 1999; Polyak *et al.*, 2007].

[40] During the mid-Pleistocene transition ~1.2 to 0.9 Ma, samples were barren or nearly barren of foraminifers suggesting several large glacial events. It is also difficult to identify glacial interglacial cycles in the proxy data for this interval despite higher sedimentation rates [O'Regan *et al.*, 2008]. This suggests that variability in the depositional

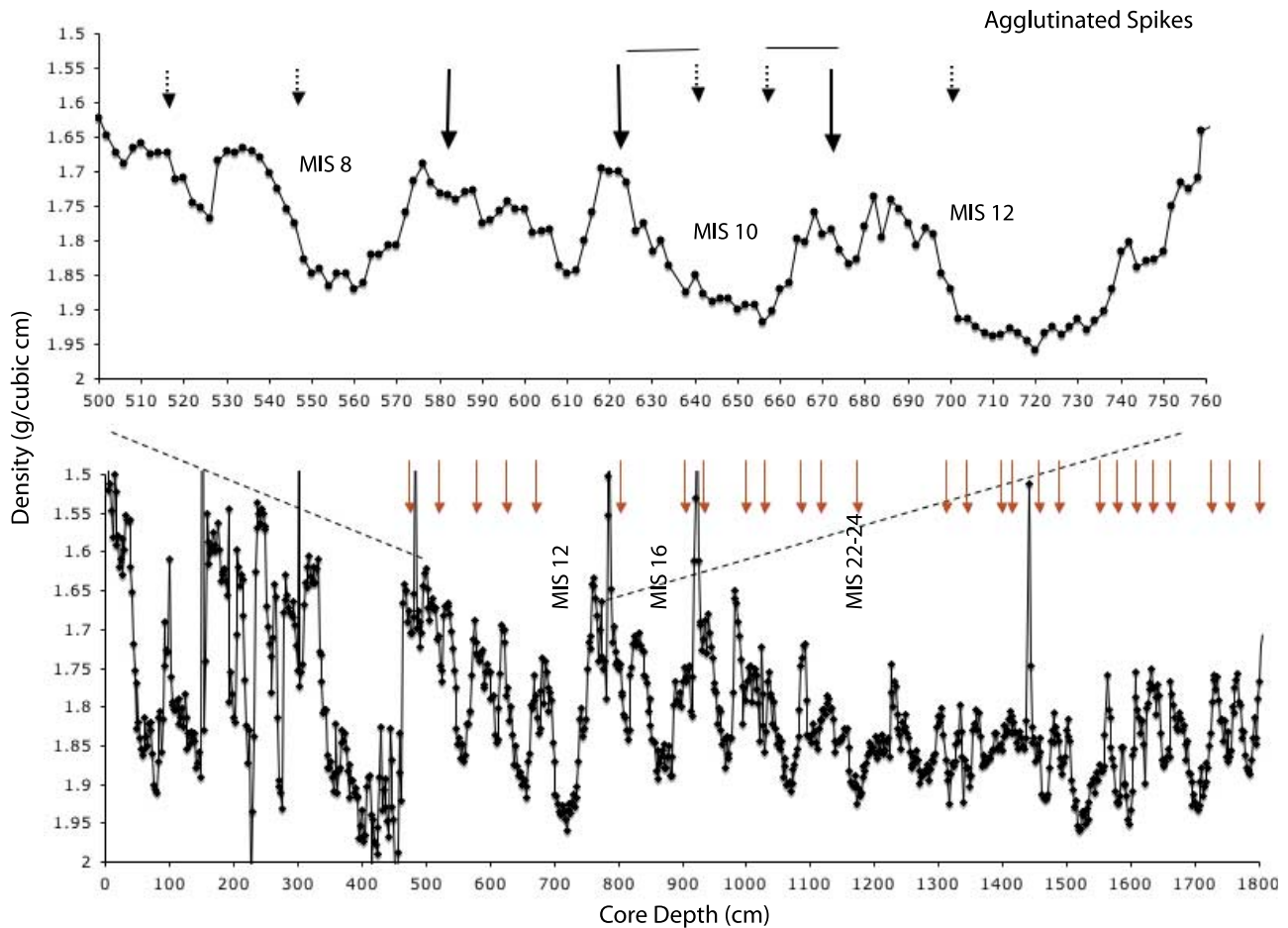


Figure 5. (bottom) Sediment bulk density for composite ACEX record. Interglacials are generally characterized by low-density intervals; glacials have high density. Red arrows indicate 27 intervals with ABF exceeding five specimens per gram. (top) Details of MIS 7–13. Larger arrows indicate ABF densities >10 specimens per gram, smaller arrows indicate $5\text{--}10\text{ gram}^{-1}$ (horizontal line between arrows indicates moderate abundance of ABFs). High ABF abundances are believed to signify seasonally ice-free conditions during interglacial or deglacial intervals.

regime between glacial and interglacial times may have been changed across the MPT. The early Pleistocene is characterized by agglutinated foraminiferal maxima alternating with rare-to-barren intervals that largely correspond to interglacial or deglacial intervals.

[41] While it is difficult to judge whether changes in abundance and assemblage composition represent a primary signal due to environmental conditions, or differential preservation potential (i.e., selective dissolution of agglutinated species having different wall structure, cement and texture) [Goody, 1990; Murray and Alve, 1994], these preliminary results have implications for Arctic paleoceanography and future studies.

[42] First, given the spotty occurrence of planktonic foraminifera on the Lomonosov and other Arctic ridges, it appears that future Arctic coring efforts might consider recovering greater amounts of sediment from the uppermost 20 m of section through wide diameter cores in order to obtain sufficient planktonic individuals for isotopic analyses or target regions that might preserve more calcareous taxa.

[43] Second, the transition from calcareous to agglutinated foraminiferal assemblages is a widespread feature of the uppermost 5–6 m of sediments deposited on ridges in the central and western Arctic Ocean. The apparent synchronicity of this change might be explained by oceanographic changes about 200–300 ka, either leading to more favorable habitats for calcareous taxa and/or the cessation of syndepositional dissolution of calcareous tests during interglacials. This transition occurs near the end of the well-known climatic transition called the “mid-Brunhes event (MBE).” The MBE was an extended period between $\sim 600\text{--}200$ ka of carbonate dissolution in the world’s oceans, culminating during MIS 11, related to changes in the global carbon cycle [Barker *et al.*, 2006]. Because calcareous faunas are abundant and well preserved in sediment deposited under the perennial sea ice of the current interglacial [Wollenburg and Kuhnt, 2000], the transition implies that during the Matuyama and early Brunhes, seasonally ice-free conditions preferred by many agglutinated taxa were common, particularly during interglacials. This hypothesis requires testing

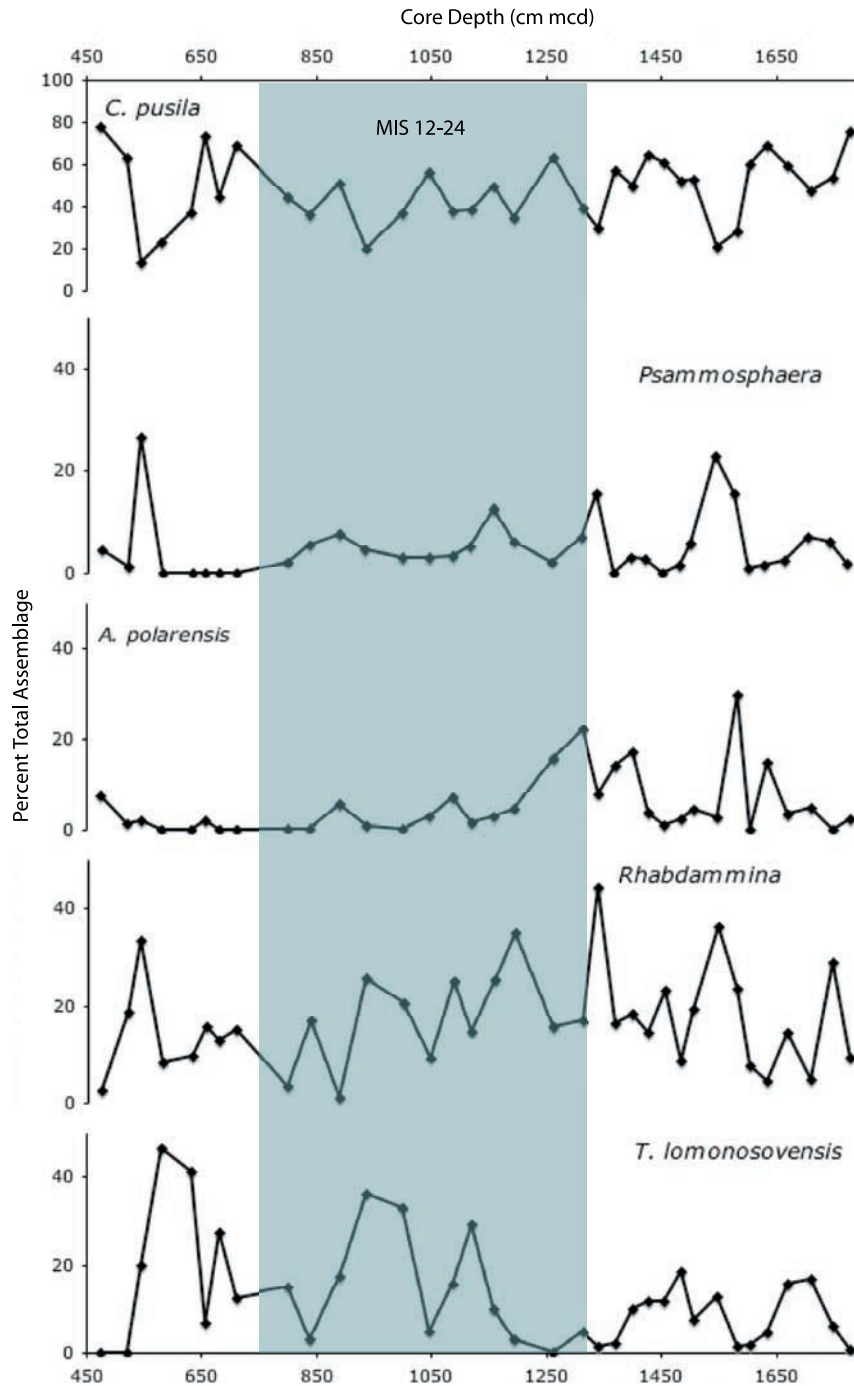


Figure 6. Quaternary agglutinated foraminiferal faunal changes in ACEX 4C. Mid-Pleistocene transition is shown by shaded area.

using the ecology and preservation potential of individual species.

[44] An alternative hypothesis to explain the calcareous-ABF pattern is that postdepositional dissolution by pore water geochemical processes operating over a wide area of the Arctic may have destroyed calcareous taxa and perhaps also some carbonate-cemented agglutinated species. Prelim-

inary pore water geochemical analyses conducted during the ACEX cruise offer clues that the transition may be a postdepositional artifact of dissolution in Arctic sediments. Alkalinity peaks about 4.0 mcd at values from 2.7 to 3 mM before falling to <2.5 mM below 15.0 mcd [Backman et al., 2006]. Measured pH values also fall gradually from near 7.6 in the uppermost intervals of the ACEX section to 7.2 near

50 mcd. Geochemical alteration is also suggested by the first peaks in solid-phase manganese about 1.5–2.0 mcd, which is related to precipitation of manganese oxides. Manganese peaks were interpreted by *Jakobsson et al.* [2000] to represent interglacial periods of well-ventilated bottom water and reduced sea ice cover. Syndepositional dissolution related to organic matter influx, corrosive bottom water and long-term pore water geochemical processes are not necessarily exclusive of one another.

[45] Third, the dominance of agglutinated foraminifers in distinct thin intervals in ACEX 4C below 6.0 mcd and at other Arctic sites resembles a characteristic feature of Cenozoic sediments deposited along high-latitude continental margins and, to a lesser extent, some abyssal plain environments. For example, pre-Neogene “flysch-type” facies have been interpreted to signify rapid sedimentation in corrosive bottom waters [*Gradstein and Berggren*, 1981; *Miller et al.*, 1982; *Kaminski*, 1985]. *Scott* [1987] and *Kaminski et al.* [1989] argued that the disappearance of ABF assemblages in the Arctic Ocean CESAR cores from the Alpha Ridge coincided with the appearance of perennial sea ice during the mid to late Brunhes (our age estimate). As discussed above, seasonally ice-free surface conditions and corrosive bottom water are conducive for preservation of agglutinated faunas in the modern Arctic and adjacent seas.

[46] Distinct foraminiferal maxima during interglacials of the Matuyama, barren intervals during strong glacials during the MPT, and the near disappearance of ABFs at the beginning of the 100-ka cycles all suggest a qualitative relationship between ABF abundance and the progressive development of sea ice following the MPT. If the positive correlation between seasonally ice-free conditions and abundant ABFs holds as it does in both modern Arctic and pre-Neogene sediments, the ACEX record shows that early Pleistocene interglacials were characterized by seasonal sea ice and perhaps summer ice-free conditions in the central Arctic Ocean.

[47] A seasonally ice-free Arctic hypothesis is indirectly supported by recent studies of the last interglacial in high Northern Hemisphere latitudes showing even the last interglacial was warmer than the Holocene interglacial. *Overpeck et al.* [2006] and *Otto-Bliessner et al.* [2006] presented sea level and climate modeling evidence for extreme Arctic warming with a reduced Greenland ice sheet during the LIG as northern hemisphere summer insolation was higher. *Nørgaard-Pedersen et al.* [2007] showed reduced sea ice characterized parts of the Arctic off northern Ellesmere Island and Greenland during MIS 5e on the basis of multiproxy evidence from sediment cores. It is also consistent with a large body of instrumental and modeling data suggesting modern Arctic sea ice is extremely dynamic and sensitive to wind and thermal forcing over decades to centuries [*Rigor and Wallace*, 2004; *Rothrock and Zhang*, 2005]. It remains unclear what may have driven sea ice formation, however it is likely a combination of inflowing warm Atlantic water and its influence on the halocline, variability in freshwater inflow, warmer atmospheric temperatures and decreased wind [*Rigor et al.*, 2002].

[48] These patterns shed light on other aspects of Arctic paleoceanography. For example, *Kristoffersen et al.* [2004]

analyzed seabed erosion on the Lomonosov Ridge by deep-draft icebergs and concluded that icebergs, calving from the Barents shelf moved northward toward the Lomonosov Ridge, reflecting the increased advection of warm Atlantic water. They suggested that discharge of these icebergs began during the MPT and characterized deglacial periods since at least 400 ka. Improved dating is needed for deep-draft iceberg erosive features, but ACEX evidence for less extensive sea and land ice prior to the MPT is consistent with the interpretations of *Kristoffersen et al.* The ABF abundance and assemblage changes in ACEX 4C also corresponds to oceanographic changes reported from the Yermak Plateau along the eastern margin of the Arctic, where *Thiede and Myhre* [1996] and *Flower* [1997] inferred change in the Svalbard ice sheet during MIS 16–17 from isotopic and stratigraphic data from ODP Sites 910 and 911.

[49] Evidence for large changes in Arctic oceanography during the MPT is consistent with several aspects of Quaternary paleoclimate records from other regions. First, many records exhibit the development of high-amplitude orbital cycles during the MPT with MIS 11–12 representing the first high-amplitude 100-ka cycle [*Lisiecki and Raymo*, 2005; *Clark et al.*, 2006]. Deep-sea oxygen isotope records indicate that early Pleistocene ice volume changes during 41-ka obliquity cycles were about half the size of typical late Pleistocene ice volume changes equivalent to 120 m of sea level change. *Clark et al.* [2006] argued that early Pleistocene ice sheets were extensive in spatial extent but relatively thin, and that after ~900 ka, they were much thicker and glacial-interglacial 100-ka ice volume changes were greater. Thinner ice sheets during glacials of the early Pleistocene might mean less extensive ice shelves along the margins of the Arctic, and this might be manifested in the central Arctic by less extensive sea ice during this time. The extended 80-ka glacial event during MIS 22–24, emphasized by *Clark et al.* as an important feature of the MPT, coincides with nearly barren ACEX 4C sediments. In fact, nearly barren intervals occur during other strong mid-Pleistocene glacial periods MIS 16 and 12.

[50] Plio-Pleistocene climatic and oceanographic-driven changes in carbonate preservation and dissolution are also well documented in several DSDP and ODP cores from the Norwegian-Greenland Sea (NGS), with an especially strong preservation shift near 1.2–1.0 Ma [*Henrich et al.*, 2002]. Although patterns in the central Arctic should not necessarily parallel those in the NGS (i.e., oceanographic transitions may be time-transgressive), *Henrich et al.* [2002] identified short-term dissolution spikes beginning in the middle-late Pleistocene (post 1 Ma) coincident with glacial terminations. They proposed that these signified an “ice sheet collapse and meltwater lid dissolution mode” and the cessation of deep-water production in the NGS. This mode contrasts with that for interglacial periods, characterized by vigorous deepwater production in the NGS similar to that today, and, conversely, glacial intervals when less dense deep water formed contributing to glacial North Atlantic Intermediate Water. *Henrich et al.* also noted widespread diamictos and poor carbonate preservation during MIS 12 and 10.

[51] In sum, despite preservational artifacts in Arctic foraminifers, combining foraminiferal patterns with new

age models, sediment physical and magnetic properties that reflect glacial-interglacial depositional patterns and other available evidence, suggests large-scale paleoceanographic changes occurred during the Quaternary that were related to the development of sea ice, inflowing Atlantic water, and possibly large icebergs and freshwater inflow.

[52] **Acknowledgments.** We thank K. Moran, J. Backman, and the scientific and technical staff of the ACEX cruise party ECORD for their assistance and inviting our participation in the ACEX project. J. Wollenburg, L. Polyak, D. Scott, and K. Foley gave freely their data and expertise of Arctic foraminifera. T. Sakamoto, J. Pohlman, and J. Dickens provided insight into pore water and sediment geochemistry. K. Hayo, J. Dyszynski, O. Ther, and R. Escobedo provided technical and lab assistance. The manuscript benefited from reviews by H. Dowsett, M. Yasuhara, and anonymous reviewers.

References

- Aagaard, K., and E. C. Carmack (1994), The Arctic Ocean and climate: A perspective, in *The Polar Oceans and Their Role Shaping the Global Environment, Geophys. Monogr. Ser.*, vol. 85, edited by O. M. Johannessen et al., pp. 5–20, AGU, Washington, D. C.
- Backman, J., M. Jakobsson, R. Løvlie, L. Polyak, and L. A. Febo (2004), Is the central Arctic Ocean a sediment starved basin?, *Quat. Sci. Rev.*, 23, 1435–1454.
- Backman, J., K. Moran, D. B. McInroy, and L. A. Mayer (2006), Arctic Coring Expedition, *Proc. Integr. Ocean Drill. Program*, 302, doi:10.2204/iodp.proc.302.2006.
- Backman, J., et al. (2008), Age model and core-seismic integration for the Cenozoic Arctic Coring Expedition sediments from the Lomonosov Ridge, *Paleoceanography*, doi:10.1029/2007PA001476, in press.
- Barker, S., D. Archer, L. Booth, H. Elderfield, J. Henderiks, and R. E. M. Rickaby (2006), Globally increased pelagic carbonate production during the mid-Brunhes dissolution interval and the CO₂ paradox of MIS 11, *Quat. Sci. Rev.*, 25, 3278–3293.
- Beck, J. W., et al. (2001), Extremely large variations of atmospheric ¹⁴C concentration during the last glacial period, *Science*, 292, 2453–2458.
- Berger, W. A., and E. Jansen (1994), Mid-Pleistocene climate shift—The Nansen connection, in *The Polar Oceans and Their Role Shaping the Global Environment, Geophys. Monogr. Ser.*, vol. 85, edited by O. M. Johannessen et al., pp. 295–311, AGU, Washington, D. C.
- Bergsten, H. (1994), Recent benthic foraminifera of a transect from the North Pole to the Yermak Plateau, eastern central Arctic Ocean, *Mar. Geol.*, 119, 251–267.
- Bischof, J., D. L. Clark, and J.-S. Vincent (1996), Origin of ice-rafted debris: Pleistocene paleoceanography in the western Arctic Ocean, *Paleoceanography*, 11, 743–756.
- Clark, D. L. (1970), Magnetic reversals and sedimentation rates in the Arctic Basin, *Geol. Soc. Am. Bull.*, 81, 3129–3134.
- Clark, D. L. (1990), Arctic Ocean ice cover: Geologic history and climate significance, in *The Geology of North America*, vol. L, *The Arctic Ocean Region*, edited by A. Grantz et al., pp. 53–62, Geol. Soc. of Am., Boulder, Colo.
- Clark, D. L., R. R. Whitman, K. A. Morgan, and S. D. Mackay (1980), Stratigraphy and glacial-marine sediments of the Amerasian Basin, central Arctic Ocean, *Spec. Pap. Geol. Soc. Am.*, 181, 1–57.
- Clark, P. U., A. Archer, D. Pollard, J. D. Blum, J. A. Rial, V. Brovkin, A. C. Mix, N. G. Pisias, and M. Roy (2006), The middle Pleistocene transition: Characteristics, mechanisms, and implications for long-term changes in atmosphere pCO₂, *Quat. Sci. Rev.*, 25, 3150–3184.
- Cronin, T. M., T. R. Holtz, and R. C. Whatley (1994), Quaternary paleoceanography of the deep Arctic Ocean based on quantitative analysis of Ostracoda, *Mar. Geol.*, 119, 305–332.
- Darby, D., L. Polyak, and H. A. Bauch (2006), Past glacial and interglacial conditions in the Arctic Ocean and marginal seas—A review, *Prog. Oceanogr.*, 71, 129–144.
- Evans, J. R. (1998), Late Neogene agglutinated foraminifera from the central Arctic Ocean, Ph.D. thesis, Univ. Coll. London, London.
- Evans, J. R., and M. A. Kaminski (1998), Pliocene and Pleistocene chronostratigraphy and paleoenvironment of the central Arctic Ocean, using deep water agglutinated foraminifera, *Micropaleontology*, 44, 109–130.
- Evans, J. R., M. A. Kaminski, T. M. Cronin, and D. Fütterer (1995), Agglutinated foraminifera from the Lomonosov Ridge and Amundsen Basin, Arctic Ocean: Initial report on piston cores, *Mar. Micropaleontol.*, 26, 245–253.
- Eynaud, F., T. M. Cronin, S. A. Smith, J. Mavel, V. Mas, and S. Zaragosi (2008), Late Pleistocene planktonic foraminifera of the ACEX cores: The use of morphotype discrimination as a new tool in polar paleoceanography?, *Micropaleontology*, in press.
- Flower, B. P. (1997), Overconsolidated section on the Yermak Plateau, Arctic Ocean: Ice sheet grounding prior to ca. 660 ka?, *Geology*, 25(2), 147–150.
- Frank, M., J. Backman, M. Jakobsson, K. Moran, M. O'Regan, J. King, B. A. Haley, P. W. Kubik, and D. Garbe-Schönberg (2008), Beryllium isotopes in central Arctic Ocean sediments over the past 12.3 million years: Stratigraphic and paleoclimatic implications, *Paleoceanography*, 23, PA1S02, doi:10.1029/2007PA001478.
- Frederichs, T. (1995), Regional and temporal variations of rock magnetic parameters in Arctic marine sediments, *Ber. Polarforsch.*, 164, 92–141.
- Fütterer, D. K. (Ed.) (1992), ARCTIC '91: The Expedition ARK-VIII/3 of RV *Polarstern* in 1991, *Ber. Polarforsch.*, 107, 1–267.
- Goody, A. J. (1990), Recent deep-sea agglutinated foraminifera: A brief review, in *Paleoecology, Biostratigraphy, Paleoceanography and Taxonomy of Agglutinated Foraminifera*, edited by C. Hemleben et al., pp. 271–304, Kluwer Acad., Dordrecht, Netherlands.
- Gradstein, F. M., and W. A. Berggren (1981), Flynch-type agglutinated foraminiferal stratigraphy and the Maestrichtian to Paleogene history of the Labrador and North seas, *Mar. Micropaleontol.*, 6, 211–268.
- Green, K. E. (1960), Ecology of some Arctic foraminifera, *Micropaleontology*, 6, 57–78.
- Hald, M., and P. I. Steinsund (1996), Benthic foraminifera and carbonate dissolution in surface sediments of the Barents- and Kara Sea, in *Surface-Sediment Composition and Sedimentary Processes in the Central Arctic Ocean and Along the Eurasian Continental Margin, Ber. Polarforsch.*, vol. 212, edited by R. Stein et al., pp. 285–307, Alfred-Wegener-Inst. für Polar- und Meeresforsch., Bremerhaven, Germany.
- Henrich, R., K.-H. Baumann, R. Huber, and H. Meggers (2002), Carbonate preservation records of the past 3 Myr in the Norwegian-Greenland Sea and the northern North Atlantic: Implications for the history of NADW production, *Mar. Geol.*, 184, 17–39.
- Hughen, K. A., et al. (2004), Marine04 marine radiocarbon age calibration, 0–26 cal kyr BP, *Radiocarbon*, 46(3), 1059–1086.
- Ishman, S. E., L. V. Polyak, and R. Z. Poore (1996), Expanded record of Quaternary oceanographic change: Amerasian Arctic Ocean, *Geology*, 24(2), 139–142.
- Jakobsson, M., R. Løvlie, H. Al-Hanbali, E. Arnold, J. Backman, and M. Mörth (2000), Manganese and color cycles in Arctic Ocean sediments constrain Pleistocene chronology, *Geology*, 28(1), 23–26.
- Jakobsson, M., R. Løvlie, E. M. Arnold, J. Backman, L. Polyak, J.-O. Knutsen, and E. Musatov (2001), Pleistocene stratigraphy and paleoenvironmental variation from Lomonosov Ridge sediments, central Arctic Ocean, *Global Planet. Change*, 31, 1–22.
- Jakobsson, M., J. Backman, A. Murray, and R. Løvlie (2003), Optically stimulated luminescence dating supports central Arctic Ocean cm-scale sedimentation rates, *Geochim. Geophys. Geosyst.*, 4(2), 1016, doi:10.1029/2002GC000423.
- Kaminski, M. A. (1985), Evidence for control of abyssal agglutinated foraminiferal community structure by substrate disturbance: Results from the HEBBLE area, *Mar. Geol.*, 66, 113–131.
- Kaminski, M. A., F. M. Gradstein, D. B. Scott, and K. D. Mackinnon (1989), Neogene benthic foraminifer biostratigraphy and deep-water history of sites 645, 646, and 647, Baffin Bay and Labrador Sea, *Proc. Ocean Drill. Program Sci. Results*, 105, 731–756.
- Kristoffersen, Y., B. Coakley, W. Jokat, M. Edwards, H. Brekke, and J. Gjengedal (2004), Seabed erosion draft icebergs in the Eurasia Basin and the influence of Atlantic water inflow on iceberg motion?, *Paleoceanography*, 19, PA3006, doi:10.1029/2003PA000985.
- Lagoe, M. B. (1977), Recent benthic foraminifera biofacies from the central Arctic Ocean, *J. Foraminiferal Res.*, 7(2), 106–129.
- Lagoe, M. B. (1979), Recent benthic foraminiferal biofacies in the Arctic Ocean, *Micropaleontology*, 25, 214–224.
- Lisiecki, L. E., and M. E. Raymo (2005), A Pliocene-Pleistocene stack of 57 globally distributed benthic $\delta^{18}\text{O}$ records, *Paleoceanography*, 20, PA1003, doi:10.1029/2004PA001071.

- Matthiessen, J., J. Knies, N. R. Nowaczyk, and R. Stein (2001), Late Quaternary dinoflagellate cyst stratigraphy at the Eurasian continental margin, Arctic Ocean: Indications for Atlantic water inflow in the past 150,000 years, *Global Planet. Change*, *31*, 65–86.
- Miller, K. G., F. M. Gradstein, and W. A. Berggren (1982), Late Cretaceous to early Tertiary agglutinated benthic foraminifera in the Labrador Sea, *Micropaleontology*, *28*, 1–30.
- Moran, K., et al. (2006), The Cenozoic palaeoenvironment of the Arctic Ocean, *Nature*, *44*, 601–605.
- Murray, J. W., and E. Alve (1994), High diversity agglutinated foraminiferal assemblages from the NE Atlantic: Dissolution experiments, *Spec. Publ. Cushman Found. Foraminiferal Res.*, *32*, 33–51.
- Nørgaard-Pedersen, N., R. F. Spielhagen, J. Thiede, and H. Kassens (1998), Central Arctic surface ocean environment during the past 80,000 years, *Paleoceanography*, *13*, 193–204.
- Nørgaard-Pedersen, N., R. F. Spielhagen, H. Erlenkeuser, P. M. Grootes, J. Heinemeier, and J. Knies (2003), The Arctic Ocean during the Last Glacial Maximum: Atlantic and polar domains of surface water mass distribution and ice cover, *Paleoceanography*, *18*(3), 1063, doi:10.1029/2002PA000781.
- Nørgaard-Pedersen, N., N. Mikkelsen, S. J. Lassen, Y. Kristoffersen, and E. Sheldon (2007), Reduced sea ice concentrations in the Arctic Ocean during the last interglacial period revealed by sediment cores off northern Greenland, *Paleoceanography*, *22*, PA1218, doi:10.1029/2006PA001283.
- Nowaczyk, N. R., and M. Baumann (1992), Combined high-resolution magnetostratigraphy and nannofossil biostratigraphy for late Quaternary Arctic Ocean sediments, *Deep Sea Res., Part A*, *39*, suppl. 2A, S567–S601.
- O'Regan, M., J. W. King, J. Backman, M. Jakobsson, K. Moran, C. Heil, T. Sakamoto, T. Cronin, and R. Jordan (2008), Constraints on the Pleistocene chronology of sediments from the Lomonosov Ridge, *Paleoceanography*, doi:10.1029/2007PA001551, in press.
- Osterman, L. E. (1996), Pliocene and Quaternary benthic foraminifera from site 910, Yermak Plateau, *Proc. Ocean Drill. Program Sci. Results*, *151*, 187–195.
- Osterman, L. E., and D. Spiegler (1996), Agglutinated benthic foraminiferal biostratigraphy of sites 909 and 913, northern North Atlantic, *Proc. Ocean Drill. Program Sci. Results*, *151*, 169–185.
- Osterman, L. E., R. Z. Poore, and K. M. Foley (1999), Distribution of benthic foraminifera (>125 microns) in the surface sediments of the Arctic Ocean, *U.S. Geol. Surv. Bull.*, *2164*, 1–28.
- Otto-Bliesner, B. L., S. J. Marshall, J. T. Overpeck, G. H. Miller, A. Hu, and CAPE Last Interglacial Project members (2006), Simulating Arctic climate warmth and icefield retreat in the last interglaciations, *Science*, *311*, 1751–1753.
- Overpeck, J. T., B. L. Otto-Bliesner, G. H. Miller, D. R. Muhs, R. B. Alley, and J. T. Kiehl (2006), Paleoclimatic evidence for future ice-sheet instability and rapid sea-level rise, *Science*, *311*, 1747–1750.
- Peterson, B. J., J. McClelland, R. Curry, R. M. Holmes, J. E. Walsh, and K. Aagaard (2006), Trajectory shifts in the Arctic and subarctic freshwater cycle, *Science*, *313*, 1061–1066.
- Phillips, R. L., and A. Grantz (1997), Quaternary history of sea ice and paleoclimate in the Amerasian Basin, Arctic Ocean, as recorded in the cyclical strata of Northwind Ridge, *Geol. Soc. Am. Bull.*, *109*, 1101–1115.
- Phillips, R. L., and A. Grantz (2001), Regional variations in provenance and abundance of ice-rafted clasts in Arctic Ocean sediments: Implications for the configuration of late Quaternary oceanic and atmospheric circulation in the Arctic, *Mar. Geol.*, *172*, 91–115.
- Polyak, L., M. H. Edwards, B. J. Coakley, and M. Jakobsson (2001), Ice shelves in the Pleistocene Arctic Ocean inferred from glaciogenic deep-sea bedforms, *Nature*, *410*, 453–457.
- Polyak, L., W. B. Curry, D. A. Darby, J. Bischof, and T. M. Cronin (2004), Contrasting glacial/interglacial regimes in the western Arctic Ocean as exemplified by a sedimentary record from the Mendeleev Ridge, *Palaeogeogr. Palaeoclimatol. Palaeoecol.*, *203*, 73–93.
- Polyak, L., D. A. Darby, J. Bischof, and M. Jakobsson (2007), Stratigraphic constraints on late Pleistocene glacial erosion and deglaciation of the Chukchi margin, Arctic Ocean, *Quat. Res.*, *67*, 235–245.
- Poore, R. Z., R. L. Phillips, and H. J. Rieck (1993), Paleoclimate record for Northwind Ridge, western Arctic Ocean, *Paleoceanography*, *8*, 149–159.
- Poore, R. Z., S. E. Ishman, R. L. Phillips, and D. H. McNeil (1994), Quaternary stratigraphy and paleoceanography of the Canada Basin, western Arctic Ocean, *U.S. Geol. Surv. Bull.*, *2080*, 1–32.
- Poore, R. Z., L. Osterman, W. B. Curry, and R. L. Phillips (1999), Late Pleistocene and Holocene meltwater events in the western Arctic Ocean, *Geology*, *27*(8), 759–762.
- Raymo, M. E., D. W. Oppo, and W. Curry (1997), The mid-Pleistocene climate transition: A deep sea carbon isotopic perspective, *Paleoceanography*, *12*, 546–559.
- Rigor, I., J. M. Wallace, and R. L. Colony (2002), Response of sea ice to Arctic oscillation, *J. Clim.*, *15*, 2648–2663.
- Rigor, I., J. M. Wallace, and R. L. Colony (2004), Variations in the age of Arctic sea-ice and summer sea-ice extent, *Geophys. Res. Lett.*, *31*, L09401, doi:10.1029/2004GL019492.
- Rothrock, D. A., and J. Zhang (2005), Arctic Ocean sea ice volume: What explains its recent depletion, *J. Geophys. Res.*, *110*, C01002, doi:10.1029/2004JC002282.
- Schneider, D. A., J. Backman, W. B. Curry, and G. Possnert (1996), Paleomagnetic constraints on sedimentation rates in the eastern Arctic Ocean, *Quat. Res.*, *46*, 62–71.
- Schröder, C. J., D. B. Scott, and F. S. Medioli (1987), Can smaller benthic foraminifera be ignored in paleoenvironmental analyses?, *J. Foraminiferal Res.*, *17*(2), 101–105.
- Schröder-Adams, C. J., F. E. Cole, F. S. Medioli, P. J. Mudie, D. B. Scott, and L. Dobbin (1990), Recent Arctic shelf foraminifera: Seasonally ice covered vs. perennially ice covered areas, *J. Foraminiferal Res.*, *20*(1), 8–36.
- Scott, D. B. (1987), Quaternary benthic foraminifera from Deep Sea Drilling Project Sites 612 and 613, Leg 95, New Jersey transect, *Proc. Ocean Drill. Program Initial Rep.*, *95*, 313–337.
- Scott, D. B., and G. Vilks (1991), Benthic foraminifera in the surface sediments of the deep-sea Arctic Ocean, *J. Foraminiferal Res.*, *21*(1), 20–38.
- Scott, D. B., P. J. Mudie, V. Baki, K. D. Mackinnon, and F. E. Cole (1989), Biostratigraphy and late Cenozoic paleoceanography of the Arctic Ocean: Foraminiferal, lithostratigraphic, and isotopic evidence, *Geol. Soc. Am. Bull.*, *101*, 260–277.
- Serreze, M. C., M. M. Holland, and J. Stroeve (2007), Perspectives on the Arctic's shrinking sea-ice cover, *Science*, *315*, 1533–1536.
- Spielhagen, R. F., et al. (1997), Arctic Ocean evidence for late Quaternary initiation of northern Eurasian ice sheets, *Geology*, *25*(9), 783–786.
- Spielhagen, R. F., K.-H. Baumann, H. Erlenkeuser, N. R. Nowaczyk, N. Nørgaard-Pedersen, C. Vogt, and D. Weiel (2004), Arctic Ocean deep-sea record of northern Eurasian ice sheet history, *Quat. Sci. Rev.*, *23*, 1455–1483.
- Stein, R., C. Schubert, C. Vogt, and D. Fütterer (1994), Stable isotope stratigraphy, sedimentation rates, and salinity changes in the latest Pleistocene to Holocene eastern central Arctic Ocean, *Mar. Geol.*, *119*, 333–355.
- Steinsund, P. I., and M. Hald (1994), Recent calcium carbonate dissolution in the Barents Sea, paleoceanographic applications, *Mar. Geol.*, *117*, 303–316.
- Stuiver, M., and P. J. Reimer (1993), Extended ¹⁴C data base and revised CALIB 3.0 ¹⁴C age calibration program, *Radiocarbon*, *35*(1), 215–230.
- Thiede, J., and A. M. Myhre (1996), The paleoceanographic history of the North Atlantic-Arctic gateways: Synthesis of the Leg 151 drilling results, *Proc. Ocean Drill. Program Sci. Results*, *151*, 645–658.
- Voelker, A. H. L., M. Samthein, P. M. Grootes, H. Erlenkeuser, C. Laj, A. Mazaud, M.-J. Nadeau, and M. Schleicher (1998), Correlation of marine ¹⁴C ages from the Nordic Seas with the GISP2 isotope record: Implications for ¹⁴C calibration beyond 25 ka BP, *Radiocarbon*, *40*(1), 517–534.
- Wollenburg, J. E., and W. Kuhnt (2000), The response of benthic foraminifera to carbon flux and primary production in the Arctic Ocean, *Mar. Micropaleontol.*, *40*, 189–231.
- Wollenburg, J. E., and A. Mackensen (1998), Living benthic foraminifera from the central Arctic Ocean: Faunal composition, standing stock and diversity, *Mar. Micropaleontol.*, *34*, 153–185.
- Wollenburg, J. E., W. Kuhnt, and A. Mackensen (2001), Changes in Arctic paleoproductivity and hydrography during the last 145 kyr: The benthic foraminiferal record, *Paleoceanography*, *16*, 65–77.
- Wollenburg, J. E., J. Knies, and A. Mackensen (2004), High-resolution paleoproductivity fluctuations during the past 24 kyr as indicated by benthic foraminifera in the marginal Arctic Ocean, *Palaeogeogr. Palaeoclimatol. Palaeoecol.*, *204*, 209–238, doi:10.1016/S0031-0182(03)00726-0.

T. M. Cronin and S. A. Smith, 926A U.S. Geological Survey, Reston, VA 20192, USA. (tcronin@usgs.gov)

F. Eynaud, Laboratoire Environnements et Paléoenvironnements Océaniques, UMR CNRS 5805, Université Bordeaux I, Avenue des facultés, F-33405 Talence cedex, France.

J. King and M. O'Regan, Graduate School of Oceanography, University of Rhode Island, Narragansett, RI 02882, USA.